JOURNAL OF SOLID STATE CHEMISTRY 98, 269–277 (1992)

# Potential Energy Maps and $H^+$ Conduction Mechanism in $HTaWO_6 \cdot xH_2O$ Pyrochlore

M. CATTI,* C. M. MARI, AND G. VALERIO

*Dipartimento di Chimica Fisica ed Elettrochimica, Università, via Golgi 19, 20133 Milano, Italy*

Received July 30, 1991

Least-energy paths of proton in the structures of $HTaWO_6$ and $HTaWO_6 \cdot H_2O$ have been calculated by the Born model of crystal energy. The atomic charge on O and the repulsive parameters are fitted to reproduce the equilibrium crystal structure of the pyrochlore $KNbWO_6$, obtaining $z_O = -0.70\ e$. Maps of $H^+$ potential energy in the anhydrous compound show that proton hopping occurs between adjacent H sites along edges of $(Ta,W)O_6$ coordination octahedra, with a theoretical activation energy of 0.60 eV in good agreement with the experimental value (0.66 eV). In the hydrated compound the proton transfer occurs by a similar mechanism, excluding an active role of water molecules. The small experimental activation energy observed in the latter case is probably due to surface conduction induced by humidity at grain boundaries. © 1992 Academic Press, Inc.

## Introduction

Solid proton conductors are materials whose potential importance is well known for a number of applications like, e.g., high-temperature electrolysis of water and hydrogen sensors. A not very large number of substances appear to show this property so far, and the interpretation of $H^+$ conduction mechanisms is still debated. Classical hopping by thermal activation, quantum-mechanical tunneling, hydrogen-bonding (Grotthus-type), and vehicular mechanisms are the main theoretical schemes proposed (*1, 2*). However, an important point which has still to be clarified is the role of lattice $H_2O$ molecules in proton conduction, as many experimental results would indicate that crystallization water enhances the conductivity of acidic compounds with respect to the corresponding anhydrous phases. This was shown for the systems with pyrochlore structure $HSbTeO_6/HSbTeO_6 \cdot H_2O$ (*3*), $HTaWO_6/HTaWO_6 \cdot H_2O$ (*4*), and $HTaTeO_6/HTaTeO_6 \cdot H_2O$ (*5*).

In order to contribute to an understanding of this and other topics concerning the mechanism of proton mobility in pyrochlores, a theoretical study based on calculation of the potential energy hypersurface of $H^+$ has been undertaken, by using computational methods based on the Born model of crystal energy (*6*). Similar investigations had proved to be useful for interpreting mechanisms of ionic conduction, e.g., in the classic work on $Na^+$ motion in $\beta$-alumina (*7*) and in studies on oxygen (*8*) and proton (*9*) conductors with perovskite structures. A simple, qualitative analysis of the $H^+$ electrostatic energy in a hypothetical $M^{6+}O^{2-}$ pyrochlore structure was also performed (*10*) using formal ionic charges. In

* To whom correspondence should be addressed.



0022-4596/92 $5.00

the present study, repulsive as well as electrostatic contributions to the potential energy of proton are considered in the $HA^{V}M^{VI}O_6 \cdot xH_2O$ ($0 \leq x \leq 1$) system, fitting fractional atomic charges to the observed structural properties and modeling the energetic role of $H_2O$ molecules, too. The positional and substitutional disorder of the pyrochlore structure is taken into account, and suitable ordering schemes are introduced where necessary. On the other hand, owing to the small size and lack of electron cloud of the $H^+$ ion, effects of positional relaxation and electron polarization of the neighboring atoms are estimated to be very small and neglected, so as to achieve a much simpler theoretical approach than that required with larger and heavier ions. The aim of this work is not only to determine the mobility paths of protons in the pyrochlore structure by a topological analysis of the potential energy hypersurface, but also to derive quantitative estimates of the activation energy to be compared with experimental results, in order to discriminate between alternative mechanisms of ionic conduction.

## The Energy Model

### *Order-Disorder in the Pyrochlore Structure*

Crystal energy calculations have been carried out on the compounds $KTaWO_6$, $HTaWO_6$, and $HTaWO_6 \cdot H_2O$, characterized by a cubic structure with space group $Fd3m$ ($Z = 8$). Experimental structural data come from neutron powder diffraction refinements (*11, 12, 10*). Actually, results of the first two papers refer to $KNbWO_6$ and $DTaWO_6$, respectively, but the size differences of atom pairs Nb/Ta and D/H are too small to affect the crystal structures significantly. Both substitutional and positional disorder are present in the atomic arrangements of all three substances, and this has to be dealt with properly in the energetic modeling. Experimental structural parameters are summarized in Table I. Ta and W atoms are distributed randomly over sites 16*d* ($\frac{1}{2}$, $\frac{1}{2}$, $\frac{1}{2}$) with octahedral oxygen coordination: this disorder was approximated by considering "average" atoms named conventionally TW and characterized by electric charge $z_{TW}$ and repulsive radius $r_{TW}$ (cf. next section). On the other hand, the positional disorder cannot be simulated by an average structure in energy calculations, as this would imply nonphysical interactions between fictitious fractional atoms at very short distances. Thus appropriate ordered models have to be applied to these structures.

TABLE I

EXPERIMENTAL STRUCTURAL DATA (UNIT-CELL EDGE AND ATOMIC COORDINATES) USED FOR ENERGY CALCULATIONS

| | $KNbWO_6$[a] | $HTaWO_6$[b] | $HTaWO_6 \cdot H_2O$[b] |
|---|---|---|---|
| $a$ (Å) | 10.363 | 10.444 | 10.400 |
| $x$(O) | 0.4375 | 0.4406 | 0.4396 |
| $x$(H) | | 0.105 | 0.085 |
| $x$(OW) | | | 0.145 |
| $x$(HW) | | | 0.105 |
| $z$(HW) | | | 0.218 |
| $x$(K) | 0.0932 | | |

[a] Ref. (*11*).
[b] Ref. (*10*).

In $KTaWO_6$, one-fourth of positions 32*e* ($x$, $x$, $x$) is occupied statistically by K; so K atoms were ordered over 8 out of the 32 available sites, destroying the symmetry operations which generate the other 24 ones. Only the threefold axes, inversion center, and $F$ lattice translations were left. The same type of disorder is shown in $HTaWO_6 \cdot H_2O$ by the O atom of $H_2O$, while the water H atoms are distributed randomly over one-sixth of positions 96*g* ($x$, $x$, $z$) (for each water molecule, the two H are disordered over three sites related by the threefold axis). Thus all space group operations but

the symmetry center and $F$ translations had to be removed for a full ordering of $H_2O$ molecules. The acidic H atom as well is affected by positional disorder over 8 out of $48f$ $(x, \frac{1}{8}, \frac{1}{8})$ sites both in $HTaWO_6$ and in $HTaWO_6 \cdot H_2O$. In this way the empty H sites (vacancies) are provided, which make a hopping mechanism feasible for proton conduction in the anhydrous phase. However, no explicit ordering is needed in this case, as the potential energy of the proton is calculated for any point in the unit cell without including any other acidic H atoms in fixed positions.

*Optimization of the Interatomic Potential*

Interactions between atoms at distance $r_{ij}$ are accounted for by a Born–Mayer-type two-body potential,

$$E_{ij} = e^2 z_i z_j / r_{ij} + b \exp[(r_i + r_j - r_{ij})/\rho], \quad (1)$$

where $e$ is the electron charge, $z_i$ and $r_i$ are the charge (in units of $e$) and repulsive radius, respectively, of atom $i$, $\rho$ is the hardness parameter of repulsion forces, and $b$ is a dimensional factor equal to $10^{-19}$ J. Lattice sums over atom pairs are calculated by the fast-converging Ewald series for the electrostatic term (*13*) and by direct summation for the short-range exponential term. Deviations from ideal ionicity of the TW–O bond character are taken into account by assuming fractional atomic charges $z_O$ and $z_{TW}$; the charge of the acidic H atom, on the other hand, must take the formal value $+1$ in order to model a mobile proton in the structure. Thus, electroneutrality requires that $2z_{TW} + 6z_O = -1$, and $z_O$ is chosen as the only independent charge to be determined. The other unknown quantities in the potential are the repulsive radii $r_O$ and $r_{TW}$, and the hardness parameter $\rho$.

These four parameters were optimized for the anhydrous pyrochlore by fitting the minimum-energy crystal structure to the experimental one. Instead of $HTaWO_6$, the potassium pyrochlore $KTaWO_6$ was considered, because here all oxygen atoms of the octahedral framework $[TaWO_6]^-$ are chemically equivalent with equal charges. This simulates reasonably a $H^+[TaWO_6]^-$ structure where the acidic H is not bonded to any particular O atom but is mobile as in the conduction process. The five structural variables $\tau_i$ of $KTaWO_6$ were considered: the edge $(a)$ and angle $(\alpha)$ of the unit cell, and the independent atomic coordinates $x$(TW), $x$(O), and $y$(O). By a least-squares version of the minimum energy (or zero force principle) (*14*), the quantity $\Delta = \sum_{i=1}^{5} w_i(\partial E/\partial \tau_i)^2$ is required to be a minimum, where $w_i$ are dimensional coefficients. The energy derivatives were calculated analytically (*6*), and the parameters of K were fixed to $z_K = 1$ and $r_K = r_O + 0.07$ Å, so as to reproduce the difference of corresponding ionic radii.

TABLE II

OPTIMIZED ATOMIC CHARGES ($z_i$), REPULSIVE RADII ($r_i$), AND HARDNESS PARAMETER $\rho$ USED IN THE ENERGY EXPRESSION [Eq. (1)]

| | | |
|---|---|---|
| $z_O = -0.70\ e$ | $r_O = 1.17$ Å | $\rho = 0.25$ Å |
| $z_{TW} = 1.60\ e$ | $r_{TW} = 0.41$ Å | |

*Note.* For the $H_2O$ molecule, see the text.

As $\Delta = \Delta(z_O, r_O, r_{TW}, \rho)$, a numerical search of $\Delta$ minimum yielded the optimized values of the four parameters (Table II). The oxygen charge was determined with a good accuracy, as can be estimated by the steep slope of the $\Delta(z_O)$ curve in the neighborhood of its minimum point (Fig. 1). A much flatter minimum is obtained, on the other hand, with respect to the repulsive radii $r_O$ and $r_{TW}$. The small value determined for $z_O$, compared to the formal oxygen charge $-2e$, indicates a substantial covalent contribution in the Ta–O and W–O bonds, consistent with the high oxidation states of these metal atoms.

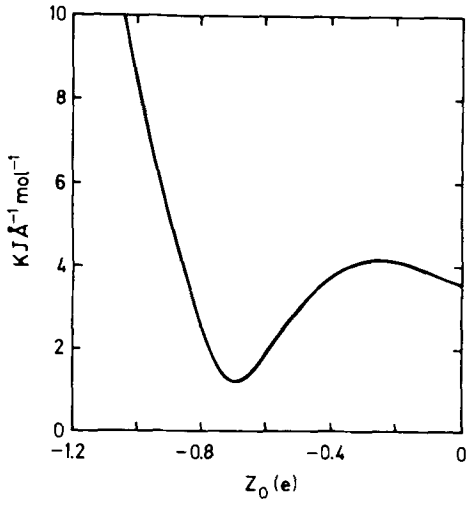


FIG. 1. Root-mean-square-value Δ of the energy derivatives with respect to structural variables vs oxygen charge.

## Results and Discussion

### *Proton Least-Energy Paths in $HTaWO_6$*

In the anhydrous pyrochlore the most probable mechanism for proton transport is thermally activated hopping between adjacent 48*f* sites at 2.628 Å. Each $(TW)O_6$ coordination octahedron is slightly stretched along a threefold axis, so that the two faces normal to it are contoured by six short edges (2.724 Å), while the other six edges are longer (2.785 Å). Only the H sites close to O atoms separated by longer edges are near enough (2.628 Å) for proton hopping, while those corresponding to short edges are quite off from each other (Fig. 2). However, the permitted edges are connected so as to provide a continuous path for proton hopping throughout the whole crystal structure. This interpretation scheme can be confirmed or discredited by a calculation of the proton potential energy as a function of $(x, y, z)$ position in the framework $[TaWO_6]^-$ with structure of $HTaWO_6$. For a positive result, plausible least-energy paths on the energy hypersurface are expected, as well as theoretical activation energies in reasonable agreement with experimental values from Arrhenius plots of electric conductivity.

This computation was performed using the empirical energy parameters reported previously, and, for the proton, a repulsive radius $r_H = 0.09$ Å, which reproduces the equilibrium bond distance in the isolated $OH^-$ group by Eq. (1). The two normal planes $(01\bar{1})$ and (100), containing the direction of the [011] open channel, were considered. The empty sites 16*c* and 8*a* in the middle of the channel, the O atoms bordering it, and the available H sites close to them are shown in Fig. 3. The potential energy surface forms wells, bumps, and saddle points in correspondence to possible proton positions, 8*a*, and 16*c* sites, respectively. Secondary saddle points appear as well. Potential minima, but not the maxima in 8*a*, were reproduced by the simple formal-charges electrostatic-only calculation (*10*). An important feature displayed in the map is the [011] elongated shape of the proton wells, indicating that the OH bending vibrations occur with low frequency along the channel direction. The smaller wells appearing farther from the channel center correspond, for symmetry reasons, to sections of the previous proton wells on the (011)

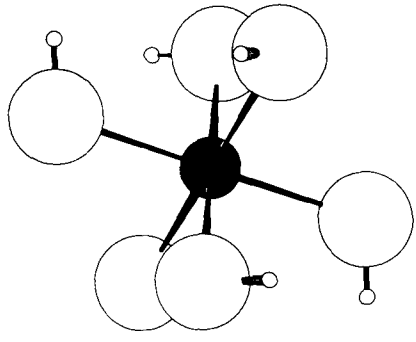

FIG. 2. Sketch of the $(Ta,W)O_6$ coordination octahedron in the pyrochlore structure, showing the six possible proton sites (small circles) close to each O atom (large open circle).

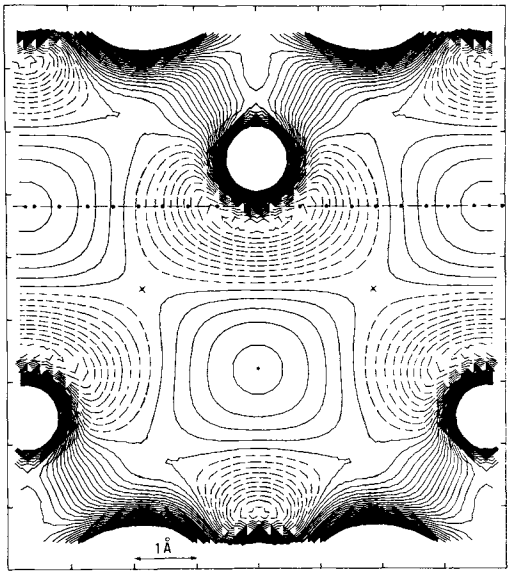


FIG. 3. Map of proton potential energy on the $(01\bar{1})$ plane for $HTaWO_6$. Horizontal and vertical axes parallel to [011] and [100] directions, respectively. Contour lines are separated by 0.1 eV; dashed lines correspond to $E \leq -0.4$ eV. Crosses and dots represent 16*c* and 8*a* sites, respectively. The dashed-dotted line shows the section of the (100) plane of Fig. 4.

plane, which is normal to that of the map and to the channel direction. Thus the two systems of wells are elongated parallel to [011] and to $[01\bar{1}]$, respectively. The thermally activated hopping of the proton in the process of ionic conduction would be triggered by the very bending mode of OH along a single channel direction.

A possible conduction mechanism on the $(01\bar{1})$ plane seems to be the proton jump from an occupied to an empty adjacent well through either the 16*c* or the secondary saddle point, with activation energies of 1.10 or 1.20 eV, respectively. However, the distance between adjacent sites on the $(01\bar{1})$ plane is very large (more than 4 Å), and the calculated activation energies are substantially greater than the measured value of 0.66 eV (*4*). Let us then consider the map of proton potential energy on the (100) plane located at $x = \frac{3}{8}$, which is normal to $(01\bar{1})$ but parallel to the [011] channel as well (Fig. 4). The 8*a* sites, four oxygen atoms belonging to two different octahedra sharing the O atom of Fig. 3 as common corner, and the shadows of TW atoms at the centers of these octahedra appear. Energy minima corresponding to possible proton equilibrium positions are found close to each oxygen atom. In the center of Fig. 4, a section of the proton potential well near the O atom of Fig. 3 can be observed: the characteristic double-minimum is due to the bowed kidney-like shape of that well. The proton can migrate on this plane by hopping from the occupied central site to one of the four empty adjacent potential wells, separated by corresponding saddle points. The proton jump is activated by OH bending vibrations along the well elongation direction. The two proton sites connected by the hopping path are close to oxygen atoms forming a long

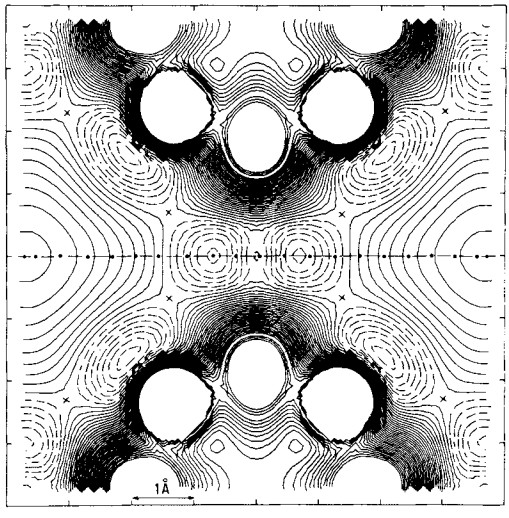


FIG. 4. Map of proton potential energy on the (100) plane for $HTaWO_6$. Horizontal and vertical axes parallel to [011] and $[01\bar{1}]$ directions, respectively. Dashed lines correspond to $E \leq -0.8$ eV. The dashed-dotted line shows the section of $(01\bar{1})$ plane of Fig. 3. Crosses and dots represent saddle points and 8*a* sites, respectively.

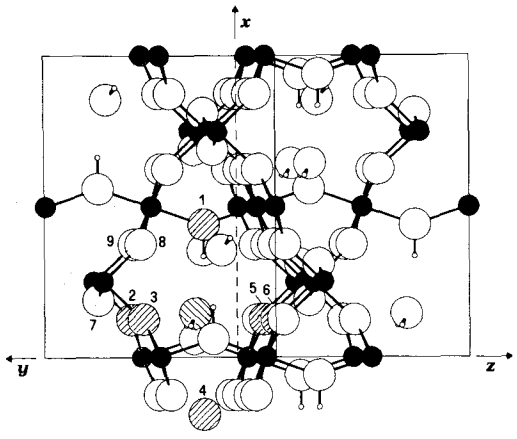


FIG. 5. Ordered structure of $HTaWO_6 \cdot H_2O$, emphasizing [011] channels and the octahedral cage surrounding a water molecule (dashed circles). Closed and open circles represent (Ta,W) and O atoms, respectively.

edge (2.785 Å) of the $(TW)O_6$ coordination octahedron, and are then at a minimum distance of 2.628 Å. Besides, the computed activation energy (difference between saddle point and minimum point potential energies) is 0.60 eV, in good agreement with the experimental value of 0.66 eV. This confirms that proton hopping along the edges of coordination octahedra bordering the [011] channels is the correct conduction mechanism in $HTaWO_6$. The proton path is very close to the (100) or equivalent planes. Mechanisms based on conduction paths on the $(01\bar{1})$ (or equivalent) planes are much less likely and should be discarded.

### *$H^+$ Conduction Mechanism in $HTaWO_6 \cdot H_2O$*

By simple inspection of the structural environment of the water molecule in the hydrated pyrochlore (Fig. 5), important conclusions can be drawn about the process of proton transfer in this compound. The OW oxygen atom of $H_2O$ is slightly shifted, along a threefold axis, from the 8*a* site at the center of a regular octahedron of acidic O atoms (distant 3.272 Å). Thus OW lies at 3.078 and at 3.492 Å from two sets (O′ and O″, 1–2–3 and 4–5–6 in Fig. 5) of three vertices, respectively. Its next neighbors are another triplet of O atoms at 3.415 Å (7–8–9 in Fig. 5), lying outside the octahedron. The $H_2O$ molecule donates very weak hydrogen bonds to two of the three O′ atoms (HW···O′ is 2.323 Å long, with the OW–HW···O′ angle of 135°) and is acceptor of another H bond donated by the acidic hydrogen of the third O′ atom (H···OW is 1.998 Å with a O′–H···OW angle of 172°). Of course the rotational disorder of $H_2O$ around the threefold axis, coupled with disorder of acidic H atoms, can cause the three hydrogen bonds to exchange with one another. The distance between any of the three possible HW positions close to OW and the acidic H site close to the nearest O′ atom is 1.252 Å; this is probably too large for quantum tunneling of the proton, while a $H^+$ transfer between the H and HW sites by classical hopping cannot be ruled out. Such a process would involve the temporary formation of a hydronium ion $H_3O^+$, with subsequent release of one proton to an adjacent O′ acidic oxygen, and a net transfer of $H^+$ between two O corners of the octahedral cage surrounding $H_2O$. By taking into account the disorder of OW itself over four positions around the 8*a* sites, all the six O atoms of the octahedron may be involved in the process.

However, the important point is that the octahedral cages in the pyrochlore structure are isolated: every acidic O atom is the corner of a single cage and can then exchange protons with a single water molecule. Therefore the Grotthus-type proton transfer cannot propagate through the whole crystal, but must be necessarily associated with proton hopping between adjacent acidic oxygens (just as in the anhydrous pyrochlore), to provide a link between different octahedral cages.

Thus the following conclusions can be de-

rived. Let us call $E_G$ the activation energy of the Grotthus-type proton transfer, controlled by hopping between H and HW sites (I), and $E_H$ the activation energy of proton hopping between acidic H sites (II). If $E_G > E_H$, then Grotthus conduction does not occur, and the only mechanism of proton motion in the hydrated pyrochlore is the same as in the anhydrous compound (II). If $E_G < E_H$, both mechanisms may cooperate in the hydrated compound, but the overall proton conductivity is determined by the slow step (II), and again the effective activation energy should correspond to that of the anhydrous pyrochlore.

Though hardly relevant for bulk conductivity, the feasibility of proton transfer between acidic O and $H_2O$ has been investigated by the same methods of potential energy calculations used for $HTaWO_6$. The contribution of water molecules to the atom–atom potential was taken into account by assuming a simple point-charge model for $H_2O$, with $z_{OW}$ located on the oxygen and $z_{HW} = -z_{OW}/2$ on each of the two hydrogen atoms. The appropriate $z_{OW}$ value to reproduce the experimental molecular electric dipole moment of 1.82 D would be $-0.67\ e$. On the other hand, several quantum-mechanical SCF calculations of the oxygen charge of water are available in the literature; using an extended 6-31G** Gaussian basis set, the values $-0.674$ and $-0.786\ e$ were obtained (*15*) by a Mulliken population scheme and by a fitting to the molecular electrostatic potential, respectively. Other reliable literature values are in the range $-0.6$ to $-0.8\ e$. The effect of the water oxygen charge on the proton potential energy in the $[TaWO_6]^- \cdot H_2O$ framework was studied by computing the energy maps on the $(01\bar{1})$ plane for different values of $z_{OW}$. It turns out that for $z_{OW} = -0.65\ e$ a double minimum potential well is observed between the acidic O atom and the oxygen OW of $H_2O$, while for larger or smaller (in modulus) charges a very broad single minimum appears slightly displaced toward OW or O, respectively. This would indicate that for $z_{OW} \approx z_O$ the acidic proton can transfer easily between the two oxygen atoms.

However, no experimental evidence for the presence of $H_3O^+$ ions in the structure of $HTaWO_6 \cdot H_2O$ is given by either neutron diffraction (*10*) or solid-state NMR (*16*) studies. Thus probably the charge distribution on OW atoms is critical and should be determined by methods accounting for the crystalline environment of water molecules. Besides, the experimental geometry of the $H_2O$ molecule in this structure (*10*), used for all calculations, shows an H–O–H angle of 120°, which is unusually larger than normally observed values. For these reasons an optimization of the oxygen charge $z_{OW}$ of $H_2O$ was attempted, fitting $z_{OW}$ to the equilibrium structure of $HTaWO_6 \cdot H_2O$ in a similar way to that used for the determining $z_O$ in the anhydrous compound. The $H_2O$ molecule was treated as a rigid group with three orientational and three translational degrees of freedom. By adding the unit cell constants $a$ and $\alpha$, eight structural variables $\tau_i$ were obtained for calculation of energy derivatives using the rigid group formalism (*14*). The energy parameters of O and TW and the $\rho$ value were kept at values optimized on $KTaWO_6$. By minimizing the mean square deviation $\Delta$ as a function of $z_{OW}$, a poorly defined minimum was found for $z_{OW} = -0.20\ e$. This charge is certainly too low, but would show at least that $z_{OW}$ in this particular structure tends to be substantially lower than the charge $z_O$ on acidic oxygens, in accordance with the apparent instability of $H_3O^+$ species.

Thus a charge of $-0.60\ e$ was chosen for OW, at the lower end of quantum determined values and consistent with no observed formation of hydronium ions. Maps of proton potential energy were computed on the $(01\bar{1})$ and (100) planes of the pyrochlore structure, and they are shown in Figs. 6 and 7, respectively. As discussed above,

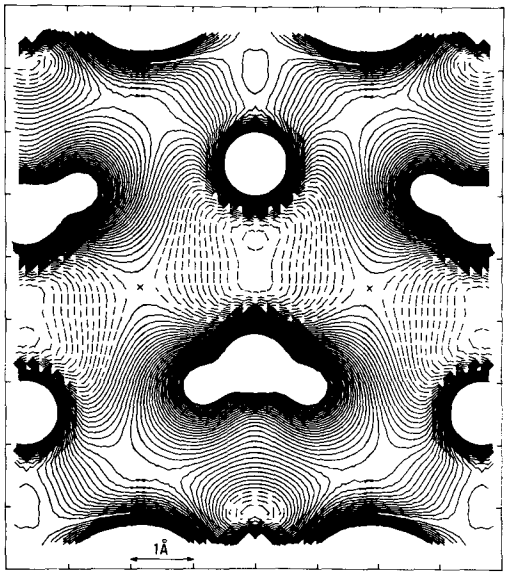


FIG. 6. Map of proton potential energy on the $(01\bar{1})$ plane for $HTaWO_6 \cdot H_2O$, with $z_{OW} = -0.60$ e. Dashed lines correspond to $E \leq -0.8$ eV.

the limiting step of proton mobility through the crystal is hopping between acidic H sites distant 2.666 Å, just as in the anhydrous compound, and the water molecules do not play an active role. By comparing Figs. 7 and 4, ordered $H_2O$ molecules are seen to lower the symmetry, so that the four potential wells of H sites are no longer equivalent and proton hopping occurs toward either of the two sites farther from adjacent molecules. The activation energy turns out to be 0.70 eV, comparable with that computed for the anhydrous pyrochlore, but much larger than the experimental value of 0.22 eV determined for $HTaWO_6 \cdot H_2O$ (*4*).

Such theoretical results can be accounted for only by assuming that the measured activation energy for proton mobility is related not to a bulk structural process, but to conduction in liquid water present at the grain boundaries. This is consistent with the low activation energy (about 0.10 eV) of the latter process and with the experimental difficulty to dry the polycrystalline sample without losing the structural water as well (*4, 5*). Furthermore, by analyzing the adsorption isotherms of other hydrates like $Ce(HPO_4)_2 \cdot xH_2O$ and $V_2O_5 \cdot xH_2O$, their protonic conductivity measured by ac impedance methods was shown to be mostly contributed by surface water (*17*). Also for the hydrates $HUO_2PO_4 \cdot 4H_2O$, $Zr(HPO_4)_2 \cdot H_2O$, and $MoO_2HPO_4 \cdot H_2O$ some evidences support a surface conduction mechanism to explain the high proton mobility observed (*18, 19*).

## Conclusions

A simple Born-type theoretical model has proved to simulate successfully the least-energy paths of proton hopping in the conduction process for $HTaWO_6$. Saddle points have been detected, obtaining a reasonable quantitative agreement between calculated and experimental activation energy.

In $HTaWO_6 \cdot H_2O$ a Grotthus mechanism of proton transfer extending to the whole structure would not be possible; hopping between acidic H sites is a necessary step,

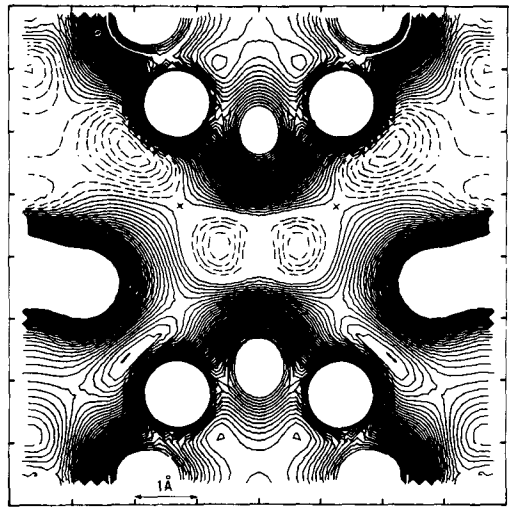


FIG. 7. Map of proton potential energy on the (100) plane for $HTaWO_6 \cdot H_2O$. Dashed lines correspond to $E \leq -0.9$ eV.

giving an activation energy similar to that of the anhydrous compound. The high conductivity measured by ac impedance technique should be related to surface liquid water, rather than to bulk processes involving structural $H_2O$ molecules. Only measurements on single crystals are able to exclude the contribution of grain boundary humidity, and in their absence a theoretical analysis can be useful to ascertain the importance of bulk effects.

## References


1. A. T. Howe and M. G. Shilton, *J. Solid State Chem.* **28,** 345 (1979).
2. K. D. Kreuer, A. Rabenau, and W. Weppner, *Angew. Chem.* **94,** 224 (1982).
3. X. Turrillas, G. Delabouglise, J. G. Joubert, T. Fournier, and J. Muller, *Solid State Ionics* **17,** 169 (1985).
4. C. M. Mari, A. Anghileri, M. Catti, and G. Chiodelli, *Solid State Ionics* **28/30,** 642 (1988).
5. M. Catti, C. M. Mari, E. Cazzanelli, and G. Mariotto, *Solid State Ionics* **40/41,** 900 (1990).
6. M. Catti, *Acta Crystallogr., Sect. A: Cryst. Phys. Diffr. Theor. Gen. Crystallogr.* **A37,** 72 (1981).
7. J. C. Wang, M. Gaffari, and Sang-il Choi, *J. Chem. Phys.* **63,** 772 (1975).
8. J. A. Kilner and R. J. Brook, *Solid State Ionics* **6,** 237 (1982).
9. A. Mitsui, M. Miyayama, and H. Yanagida, *Solid State Ionics* **22,** 213 (1987).
10. D. Groult, J. Pannetier, and B. Raveau, *J. Solid State Chem.* **41,** 277 (1982).
11. D. W. Murphy, R. J. Cava, K. Rhyne, R. S. Roth, A. Santoro, S. M. Zahurak, and J. L. Dye, *Solid State Ionics* **18/19,** 799 (1986).
12. F. J. Rotella, J. D. Jorgensen, B. Morosin, and R. M. Biefeld, *Solid State Ionics* **5,** 455 (1981).
13. M. Catti, *Acta Crystallogr., Sect. A: Cryst. Phys. Diffr. Theor. Gen. Crystallogr.* **A34,** 974 (1978).
14. M. Catti and G. Ivaldi, *Phys. Chem. Miner.* **9,** 160 (1983).
15. S. R. Cox and D. E. Williams, *J. Comput. Chem.* **2,** 304 (1981).
16. M. A. Butler and R. M. Biefeld, *Phys. Rev. B* **19,** 5455 (1979).
17. P. Barboux, R. Morineau, and J. Livage, *Solid State Ionics* **27,** 221 (1988).
18. G. Alberti, M. Casciola, and U. Costantino, *in* "Solid State Protonic Conductors II" (J. B. Goodenough, J. Jensen and M. Kleitz, Eds.), Odense Univ. Press, Odense (1985).
19. M. T. Weller and R. G. Bell, *Solid State Ionics* **35,** 79 (1989).